Computational Analysis of Effective Thermal Conductivity and Thermal Resistance of Microencapsulated Phase Change Material Coated Woven Fabric

Muhammad Owais Raza Siddiqui [a, b,*] and Danmei Sun[a]

[a]School of Textiles and Design, Heriot Watt University, TD1 3HF, UK

[b]Department of Textile Engineering, NED University of Engineering and Technology, Karachi, 75270, Pakistan

[*] Corresponding author: **Muhammad Owais Raza Siddiqui**
E-mail address: mos30@hw.ac.uk

ABSTRACT

Microencapsulated Phase change materials (MicroPCMs) have been widely used as filler material to develop thermo-regulating textile composites. Phase change materials (PCM) have unique property of latent heat that can absorb and release energy over constant temperature range. In this Work a method is developed to predict the effective thermal conductivity and thermal resistance of microencapsulated phase change material coated woven fabric via finite element analysis (FEA). For this purpose unit cell of MicroPCMs as coated material and woven fabric were developed and analysed by applying different boundary condition. Validation of the method was carried out on the basis of strong correlation in effective thermal conductivity and thermal resistance values of the MicroPCMs coated fabric between results measured from an experimental setup and the predicted values from prost-processing calculation by finite element method.

Keywords: Microencapsulated Phase change materials (MicroPCMs); Effective thermal conductivity; Thermal resistance; Finite element method

1. INTRODUCTION

Microencapsulated phase change materials (MicroPCMs) are thin wall spherical particles consisting of core phase change material (PCM) and the wall. The wall is inert and high temperature resistant polymeric material, which prevents leakage of the core material while in liquid phase. MicroPCMs are widely used to regulate the temperature and heat storage in many applications such as building materials [1], electronics [2], thermal energy storage system [3], solar heating system [4], coating of textiles [5, 6], and fibres[7, 8].

The MicroPCMs technology was first incorporated inside textile fibres in 1987 to improve their thermal performance [9] and MicroPCMs can also be incorporated in textile fabric by coating. When PCM fabric is exposed to hot environment it absorbs heat and keeps the temperature of fabric constant until PCM melts and similarly

when it is subjected to cold environment, where the temperature below the crystallization temperature of PCM it converts from liquid to solid [10]. Thermal performance of PCM fabric mainly depends on the amount of PCM used in the fabric.

Heat and moisture transfer in PCM fabric have been investigated by many researchers. In 1990, Lamb and Duffy-Morris[11] measured the heat loss through fabrics with and without PCM additives. Pause [12] investigated the development of heat and cold insulating membrane structures with phase change materials. For that he carried out research to develop a new membrane material with improved thermal properties by the application of phase change material. Nuckols [13] developed an analytical model of a diver dry suit enhanced with micro-encapsulated phase change materials to predict their thermal performances in simulated ocean environments. Kim and Cho [14] developed thermostatic garments using MicroPCMs and assessed their temperature sensing properties and compared to the garments without MicroPCMs. Ghali et al [15] studied the effect of phase change materials on clothing during periodic ventilation.

Li and Zhu [16] developed a mathematical model to predict the heat and moisture transfer through PCM textile on the basis of finite volume difference method. The purpose of that work was to develop a tool which numerically computed the distributions of temperature, moisture concentration and water content in the fibres for different amounts of PCM applied in porous textiles. Fengzhi and Yi [17] developed a mathematical model that analysed the heat and moisture transfer in porous textiles with PCM microcapsules and analysed the effect of fibre hygroscopicity on the distributions of water vapour concentration in the fabrics, water content in the fibres and on the effect of PCM microcapsule in delaying fabric temperature variation during environment transient periods.

Fengzhi [18] established a dynamic model to analyse the mechanisms of heat and moisture transfer in PCM incorporated clothing and investigated the effect of PCM distribution by considering the effect of water content on physical parameters of textiles and heat transfer with phase change. Ying et al [19] developed a dynamic mathematical model of heat and moisture transfer in multi-layer porous textiles, in which some layers incorporated PCM. A finite element volume difference scheme was used to numerically simulate the thermal regulating performance.

Bendkowska and Wrzosek [20] studied the thermoregulating properties of nonwovens treated with microencapsulated PCM and determined the temperature regulating factor and thermal resistance.

Sánchez et al [21] developed a thermoregulating textile by using PCM microcapsules through a coating technique. The thermoregulatory effect was studied by using an infrared thermography (IR) camera. Salaün et al [5] manufactured the thermoregulating textile fabric based on different mass ratio of binder to microcapsules and analysed the effect of the amount of microcapsules and binder on the thermal response of the fabric.

Alay et al [22] analysed the thermal comfort properties of the fabrics incorporating microencapsulated phase change materials (MicroPCMs) and studied the thermal conductivity and thermal resistance under steady-state condition. Yoo et al [23] investigated the thermoregulating properties of four-layer garments and analysed the effects of the number of layer and position of fabrics treated with PCM in a garment. Their work showed that the location of the PCM-treated fabric in a garment is an important factor in determining the rate of heat loss.

More recently Hu et al [24] developed an one dimensional mathematical model to analyse the thermal insulation property of protective clothing embedded with PCM for firefighters. The research was focused on temperature variation by comparing different thicknesses and position conditions of PCM in the clothing, as well as the melting state of PCM and human irreversible burns.

The aim of this work is to develop a model on the basis of finite element method to calculate the effective thermal conductivity and thermal resistance of MicroPCMs coated cotton, wool and Nomex® fabrics.

2. MATERIALS

In this study fabrics were coated both sides with MicroPCMs obtained from Microtech laboratory Inc. The fabric specifications are shown in Table 1.. MicroPCMs are composed of n-octadecane as core material and melamine formaldehyde as shell material. The properties of MicroPCMs are listed in Table 2.The core content (in percentage) of MicroPCMs can be calculated by using the following equation [25]:

$$C = \frac{\Delta H_m}{\Delta H_o} \times 100 \quad (1)$$

where C is the core content in percentage; ΔH_m and ΔH_o are the enthalpy of MicroPCMs and pure PCM respectively.
The diameter and shell thickness of MicroPCMs can be calculated by the following equations [26, 27]:

$$\left(\frac{d_p}{d_c}\right)^3 = 1 + \frac{\rho_c(1-\alpha_c)}{\rho_s \alpha_c} \quad (2)$$

$$T_S = \frac{d_p}{2}\left(1 - \sqrt[3]{\frac{C \times \rho_s}{\rho_c - C\rho_c + C\rho_s}}\right) \quad (3)$$

where d_p and d_c are the diameter of microcapsule and core, respectively; ρ_c and ρ_s are the density of core and shell, respectively; T_S is the shell thickness and α_c is the mass fraction of core.

Table 1. Fabric Specification

Specifications	Nomex® III	100 % Cotton	100% wool
Areal density (g/m^2)	170	132	130
Thickness* (mm)	0.50	0.484	0.408
Warp/Weft sett (per inch)	59/59	65/55	70/45
Warp/Weft Yarn linear density (Tex)	33.3/33.3	25.5/25.5	27.8/27.8

*Fabric thickness was the thickness without MicroPCMs coating

Table 2. Physical properties of MicroPCMs

Properties of microcapsules	
Capsule composition	85-90% wt.% PCM
Core material	n-octadecane
Shell material	Melamine Formaldehyde
Particle size	17-20 (µm)
Melting point	28.2 °C
Heat of Fusion	180-195 J/g
Specific Gravity	0.9

3. Finite Element Modelling and Simulation

In order to compute the effective thermal conductivity of MicroPCMs coated fabric a finite element model of MicroPCMs coated fabric was developed. For geometricl model generation, the SEM images of coated fabrics were analysed and it was found that the MicroPCMs were only at the surface of the fabric because it is surface coating and air is entrapped inside the yarn as shown in Figure 1.

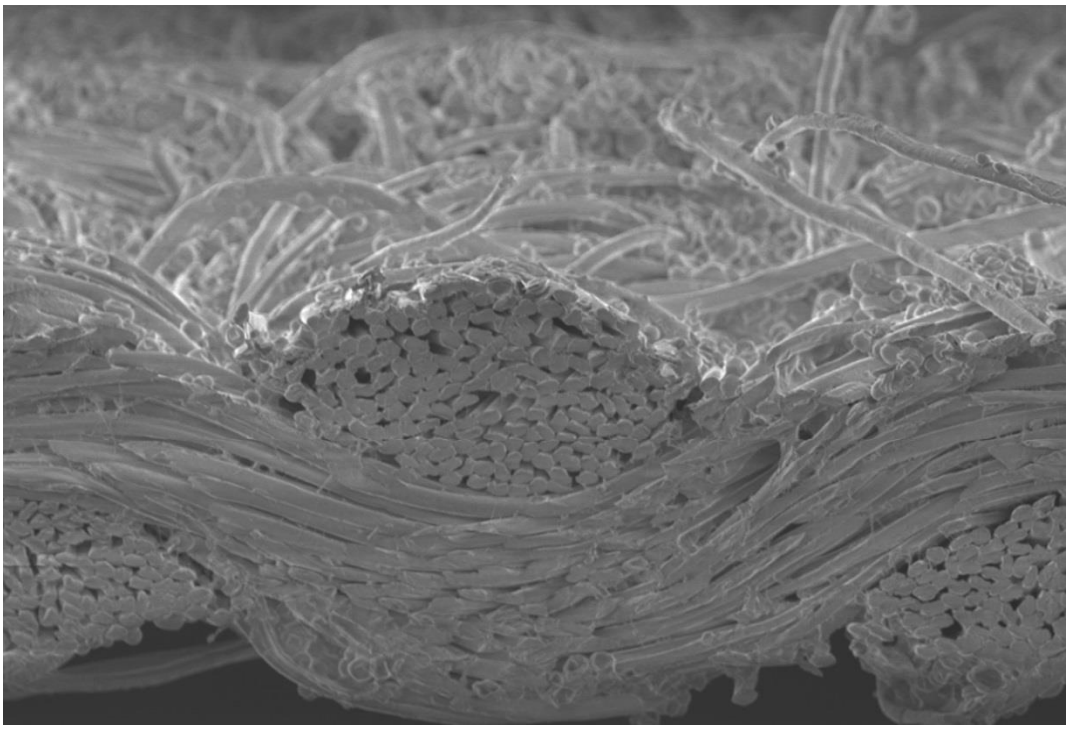

Figure 1. Micrograph of the cross-section of fabric coated MicroPCMs

For finite element modelling following steps were followed:

1) First to develop an unit cell model of MicroPCMs and binder and analyse the model.
2) Unit cell modelling of uncoated fabric.
3) Unit cell modelling of fabric with coated materials.
4) Combine the above three steps and calculate the effective thermal conductivity of MicroPCMs coated fabric.

The methods were adopted to develop the finite element model of MicroPcms coated fabric and the detailed steps were illustrated in Figure 2.

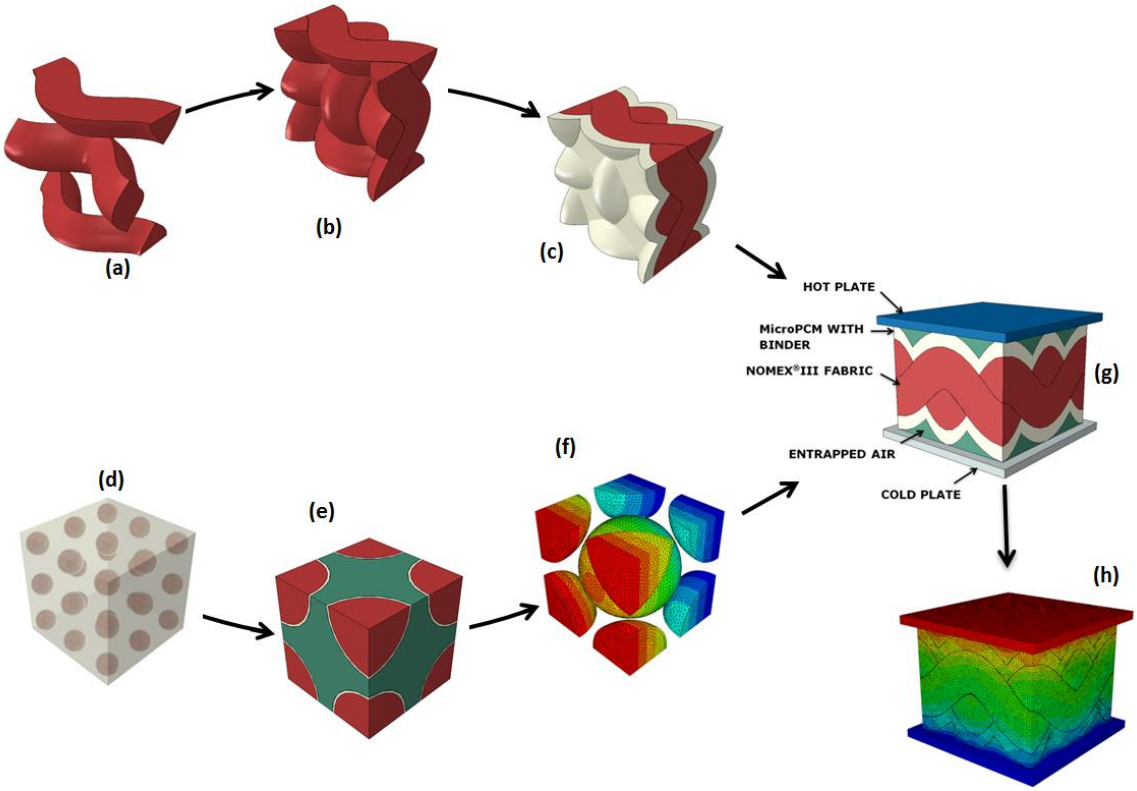

Figure 2. Stages of modelling: (a) Model of yarn; (b) Unit cell model of woven fabric only; (c) Unit cell model of woven fabric with coated material; (d) Binder and MicroPCMs composite; (e) Unit Cell model of binder and MicroPCMs composite; (f) Simulated temperature profile of binder and MicroPCMs composite; (g) Fabric composite model with bondery conditions; and (h) Simulated temperature profile of fabric composite.

3.1 Unit Cell Model of Binder and MicroPCMs Composite

The fabrics were coated with mixture of MicroPCM and binder in which contained 60% MicroPCM. Figure 3 is an unit cell model showing the components of the fabric

composite model with bindery contions. The unit cell model for binder and MicroPCM is developed by using micro-sphere filled composite material approach. The following assumptions have been taken in developing the model.

i) Acrylic binder as matrix and MicroPCMs as filler which is homogenously distributed.
ii) Only one mode of heat transfer was consider i.e. conduction
iii) No internal heat generation of the model.
iv) No PCM density variation with respect to temperature change.

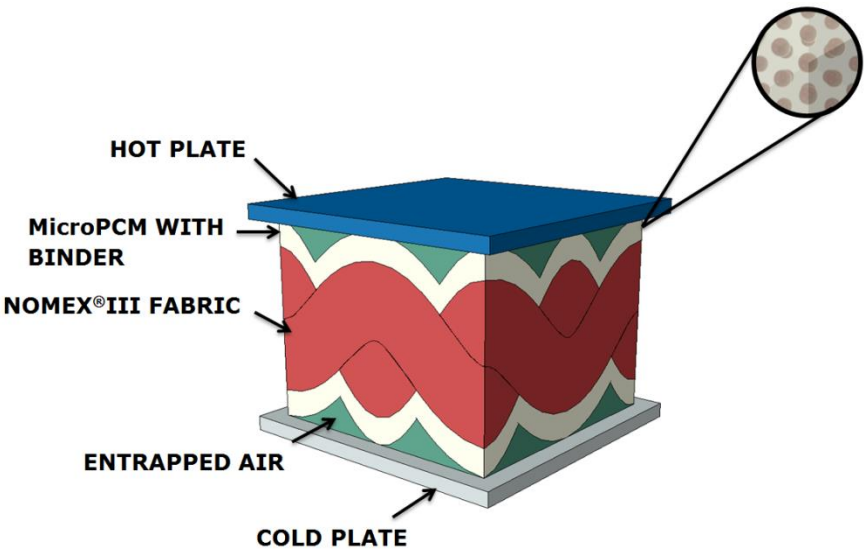

Figure 3. Experimental setup of MicroPCM coated fabric

Table 3 shows the thermo-physical properties of the core and shell of microcapsules and the actylic matrix (binder) which were used as the material properties in finite element analysis. Figure 4 presents the unit cell model of binder and MicroPCMs with 60% volume fraction of MicroPCMs. It was meshed by 4-node linear tetrahedral elements (DC3D4) with 1863 nodes and 8455 elements.

Table 3. Thermo-physical Properties

Property	n-Octadecane [16]	Melamine Formaldehyde [28]	Acrylic Binder
Density (Kg/m^3)	779	1500	1080
Specific heat (KJ/Kg.K)	1.9 (Solid) 2.2 (Liquid)	1.2	2.4
Thermal conductivity (W/m.K)	0.4 (Solid) 0.3 (Liquid)	0.5	0.155[29]
Latent Heat of Fusion (KJ/Kg)	238.76	-	-
Melting Point (˚C)	28.2	-	-

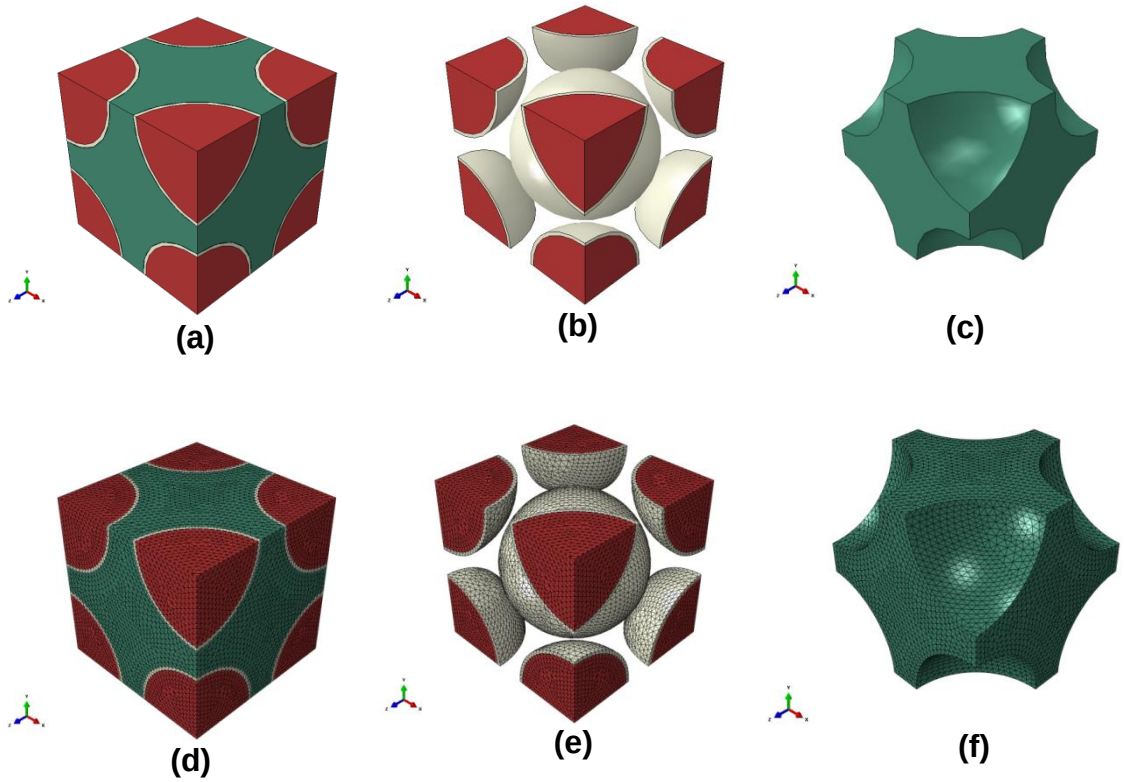

Figure 4. Unit cell model of MicroPCMs and Binder: (a) MicroPCMs with Binder; (b) MicroPCMs only; (c) Binder only; (d) (e) and (f) are Meshed unit cell.

For one dimensional heat transfer analysis the temperature specified boundary conditions was used to define the temperature for hot and cold surface and keep other surfaces insulated. Thermal effective conductivity of the binder and MicroPCMs composite can be calculated by the Fourier's law of conduction.

$$Qcond = -K_e A \frac{\Delta T}{t} \tag{4}$$

where K_e, A, ΔT and t are the effective thermal conductivity of binder and MicroPCMs, surface area, temperature gradient and thickness of the unit cell respectively.

Figure 5 illustrates contours of the MicroPCM and Acrylic binder model from post-processing calculation.

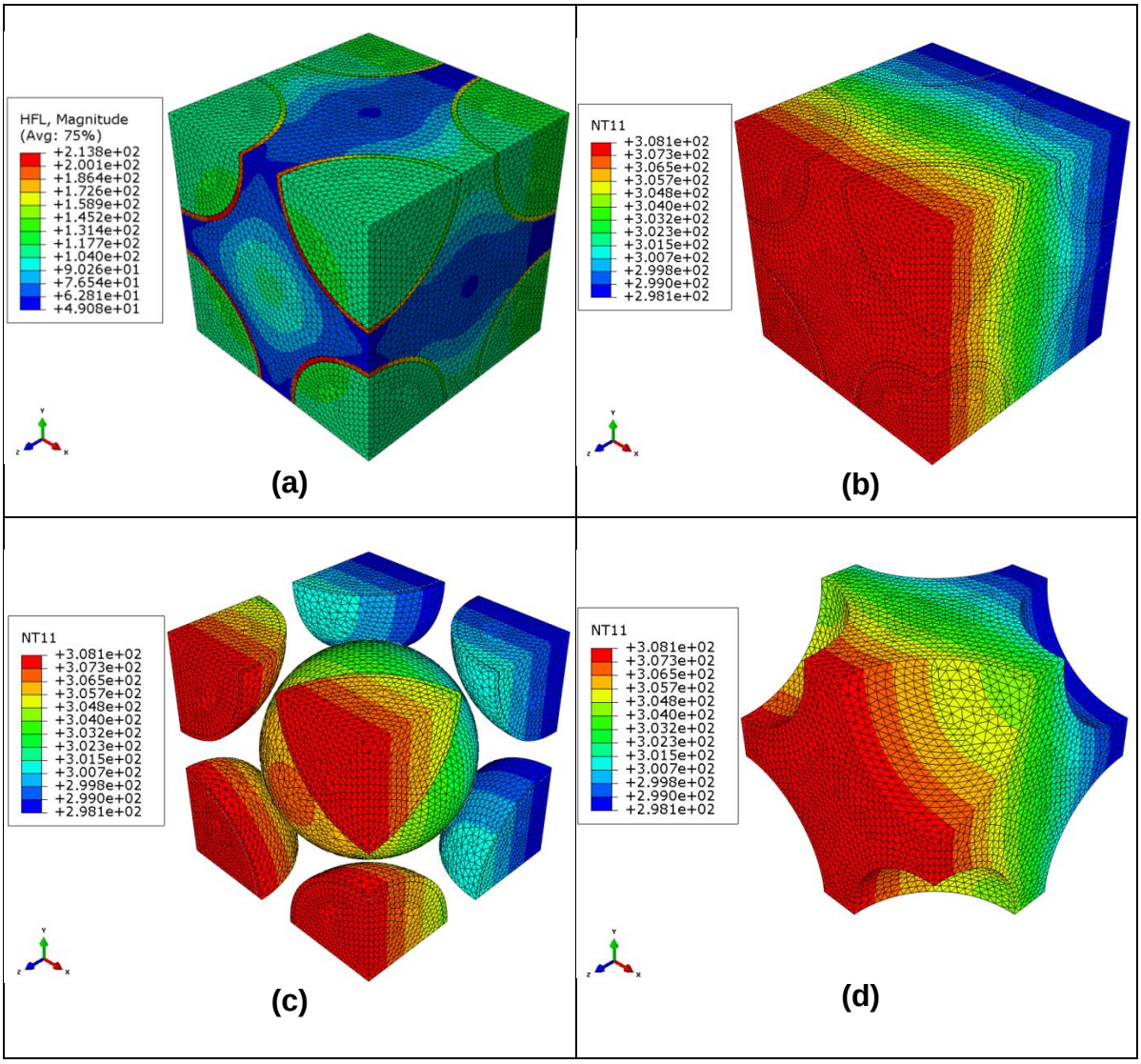

Figure 5. (a), (b) Heat Flux and temperature contour of unit cell of MicroPCMs and Binder respectively; (c) Temperature contour of MicroPCMs only; and (d) Temperature contour of Binder only.

In order to compare the results of effective thermal conductivity obtained by FEM with Maxwell model different volume fraction of MicroPCM (ϕ) was used in FEWM analysis. The results were close enough to the results obtained from Maxwell model as shown in Figure 6. The thermal conductivity of MicroPCMs was calculated by composite sphere approach [30].

$$\frac{1}{K_p d_p} = \frac{1}{K_c d_c} + \frac{d_p - d_c}{K_s d_p d_c} \tag{4}$$

where K_p , K_s and K_c are the thermal conductivity of MicroPCMs, shell and core of PCM microcapsule respectively.

The effective thermal conductivity of acrylic binder and MicoPCMs can be calculated by Maxwell model[31] by using the thermal conductivity of MicroPCMs obtained from the above Equation 4.

$$K_e = K_b \frac{2K_b + K_p + 2\phi(K_p - K_b)}{2K_b + K_p - \phi(K_p - K_b)} \tag{5}$$

where K_e is the effective thermal conductivity of binder and MicroPCMs, K_b and K_p are the thermal conductivity of binder and MicroPCMs respectively, and ϕ is the volume fraction of MicroPCMs.

Figure 6 presents the results obtained from FEM post-processing and results calculated from Maxwell model. It shows that the two methods are agreed better at lower MicroPCM volume fraction.

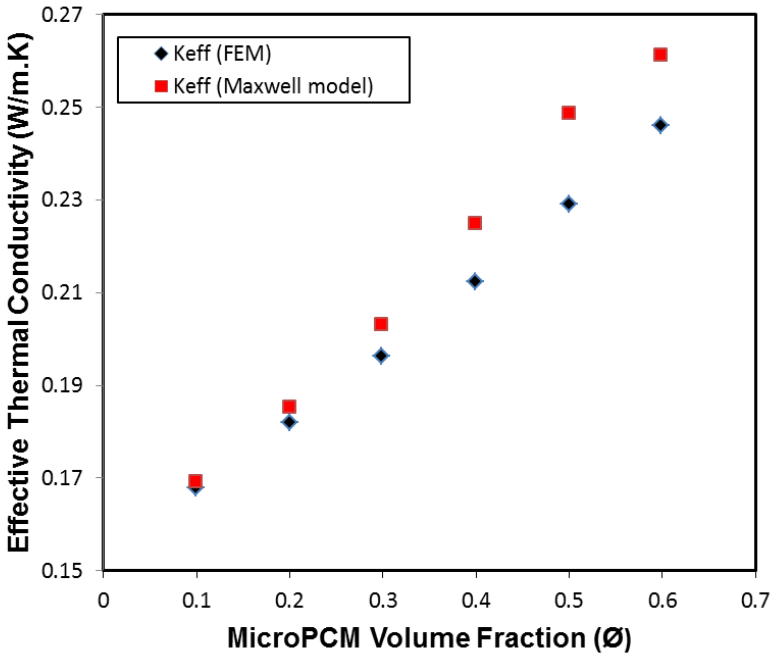

Figure 6. Results comparison between FEM and Maxwell model

3.2 Unit Cell Model of Fabric with and without coating

For the development of model of coated fabrics the following assumptions were taken when applying bondery conditions for the coated fabrics to be placed between the hot and cold plates:

i) no compression applied to fabric from the plates;
ii) entrapped air exists between the plate and fabric as shown in Figure 3; and
iii) no radiation and convection involved.

Unit cell of model of fabric was created by using the data as shown in Table 4. Yarn cross-section and dimension were obtained from the analysis of SEM images. Fabric thickness was obtained from FAST-1 under 2gf/cm^2 or 0.0196 KPa. Warp and weft spacing were calculated from warp and weft sets. Figure 7 shows the geometric and meshed model of Nomex III fabric.

Table 4. Geometric Dimensions of models

Dimensions	Nomex® III	Cotton	Wool
Warp/weft Spacing (mm)	0.431/0.431	0.390/0.462	0.363/0.564
Warp/weft width (mm)	0.337/0.337	0.26/0.277	0.3/0.33
Fabric thickness (mm)	0.68	0.575	0.56
Total length of unit cell (mm)	0.862	0.924	1.128
Total width of unit cell (mm)	0.862	0.78	0.726
Unit cell volume (mm^3)	0.505	0.4144	0.458

(Move Figure 7 to here)

Table 5 shows the thermal properties of fibres which were used in the analysis of effective thermal conductivity of coated fabrics. In order to determine the effective thermal conductivity of coated fabric there is need to calculate the axial and transverse thermal conductivity of yarn. The material for yarn is considered as orthotropic in nature so the yarn thermal conductivity along and transverse to the fibres as shown in Table 6 which were calculated by equations (6) and (7).:

$$K_{ya} = K_{fa}V_{fy} + K_{air}(1-V_{fy}) \tag{6}$$

$$K_{yt} = \frac{K_{ft}K_{air}}{V_{fy}K_{air} + (1-V_{fy})K_{ft}} \tag{7}$$

where K_{ya} and K_{yt} are the yarn thermal conductivity along the fibres and transverse to the fibres, respectively; K_{fa} and K_{ft} are the thermal conductivity of fibre in axial and

transverse directions, respectively; K_{air} is thermal conductivity of air; and V_{fy} is the yarn fibre volume fraction.

Table 5. Fibre Specifications

Property	Symbol	Nomex® III[32]	Cotton[33]	Wool[33]
Fibre density (Kg/m^3)	ρ_f	1380	1520	1310
Fibre thermal conductivity	K_{fa}	1.3[a]	2.88	0.48
(W/m.k)	K_{ft}	0.3	0.243	0.165
Fibre specific heat (J/Kg.K)	C_{pf}	1200	1350	1360

[a] consider axial thermal conductivity value 10 times than the transverse [34]

Table 6: Fibre volume fraction and yarn thermal conductivity

Fabrics	Yarn Fibre Volume Fraction, V_{fy} (%)	Fibre volume fraction of unit cell, V_f (%)	Yarn thermal Conductivity in axial direction, K_{ya} (W/m.K)	Yarn thermal Conductivity in transverse direction, K_{yt} (W/m.K)
Nomex® III	40.00	18.12	0.5356	0.0382
Cotton	38.33	15.07	1.1199	0.0395
Wool	51.00	17.7	0.2575	0.0456

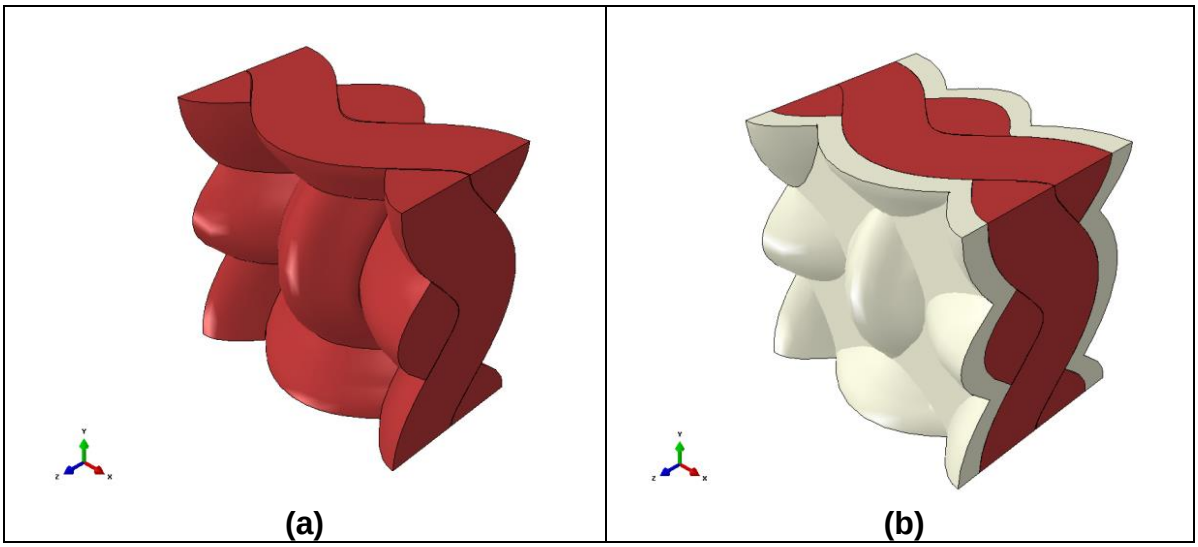

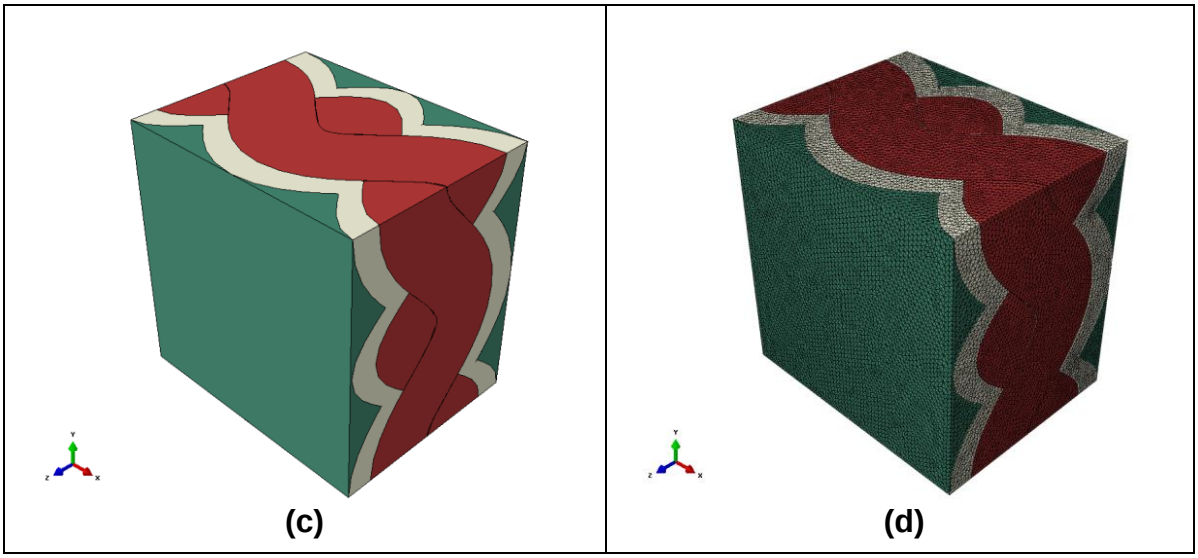

Figure 7. (a) Unit cell model of Nomex® III fabric without MicroPCMs; (b) unit cell model of Nomex® III fabric with MicroPCMs only; (c) unit cell model of Nomex® III fabric with MicroPCMs and air fluid matrix; and (d) Meshed unit cell model of Nomex® III fabric with MicroPCMs and air fluid matrix.

The local thermal conductivity tensor for material is described as:

$$K = \begin{bmatrix} K_{11} & 0 & 0 \\ 0 & K_{22} & 0 \\ 0 & 0 & K_{33} \end{bmatrix} \tag{8}$$

where K_{11} is the thermal conductivity along the fibre direction and $K_{22} = K_{33}$ are the thermal conductivity perpendicular to the fibre direction.

The calculated thermal conductivity of yarn along fibre ($K_{11} = K_{ya}$) and transverse ($K_{22} = K_{33} = K_{yt}$) to the fibre direction were used as material input parameters in Abaqus. Due to the crimps of the yarn in fabric the yarns move up and down, as a result the material principal axes may vary from point to point. Therefore coordinate of material principal axes transform by using coordinate transformation matrix.

The effective thermal conductivity of MicroPCMs and binder was obtained from the unit cell of MicroPCMs and binder were used as input material property for the coating section as shown in Figure 7 (b). The thermal conductivity of air 0.026 w/m.K was used as input material property for air fluid matrix section.

A unit cell of MicroPCMs coated fabrics were meshed by 4-node linear tetrahedral elements (DC3D4). In order to determine the effective thermal conductivity of MicroPCMs coated across the transverse direction, temperature specified boundary condition were used for one dimensional heat flow. For that purpose temperature

gradient is applied at the face and back side of the unit cell,assumming surfaces remain insulated.

Figure 8 shows the temperature distribution of Nomex® III fabric with MicroPCMs and air fluid matrix. Figure 9 shows the heat flux distribution of MicroPCMs coated Nomex® III, cotton and wool fabrics. The effective thermal conductivity across the thickness of unit cell can be determined by the equation:

$$K_{eff} = Q_z \frac{t}{\Delta T_z} \tag{9}$$

where Q_z and ΔT_z are the overall heat flux value and the temperature difference in z-direction (fabric thickness direction) respectively.

The detailed calculation of Q_z can be found in reference [35]. Table 7 shows the FE model predicted thermal conductivity of MicroPCMs coated fabric.

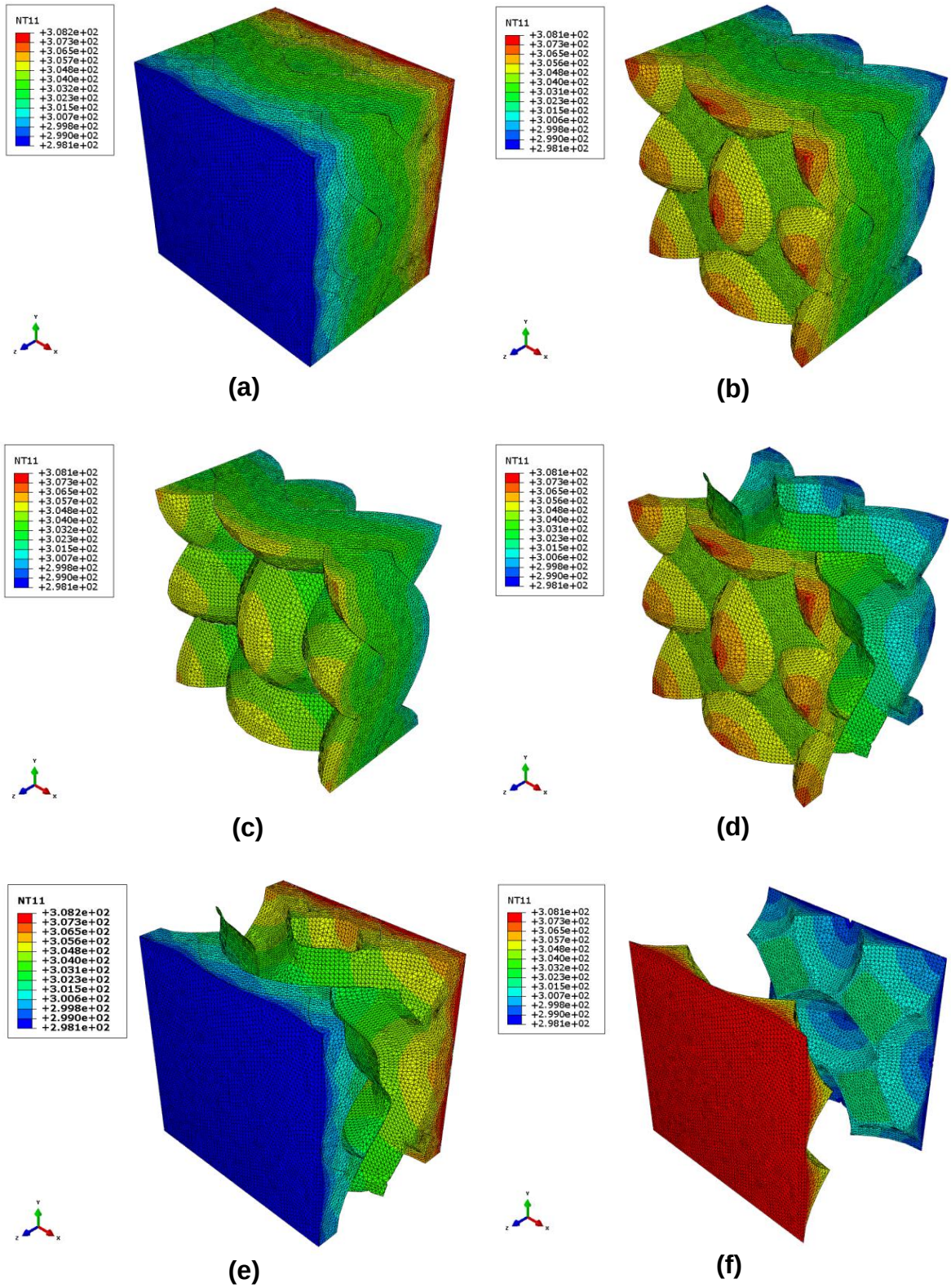

Figure 8. Temperature contour of MicroPCMs coated Nomex® III fabric.

Figure 9. Heat Flux Contour of MicroPCMs coated fabric: (a) MicoPCMs Coated

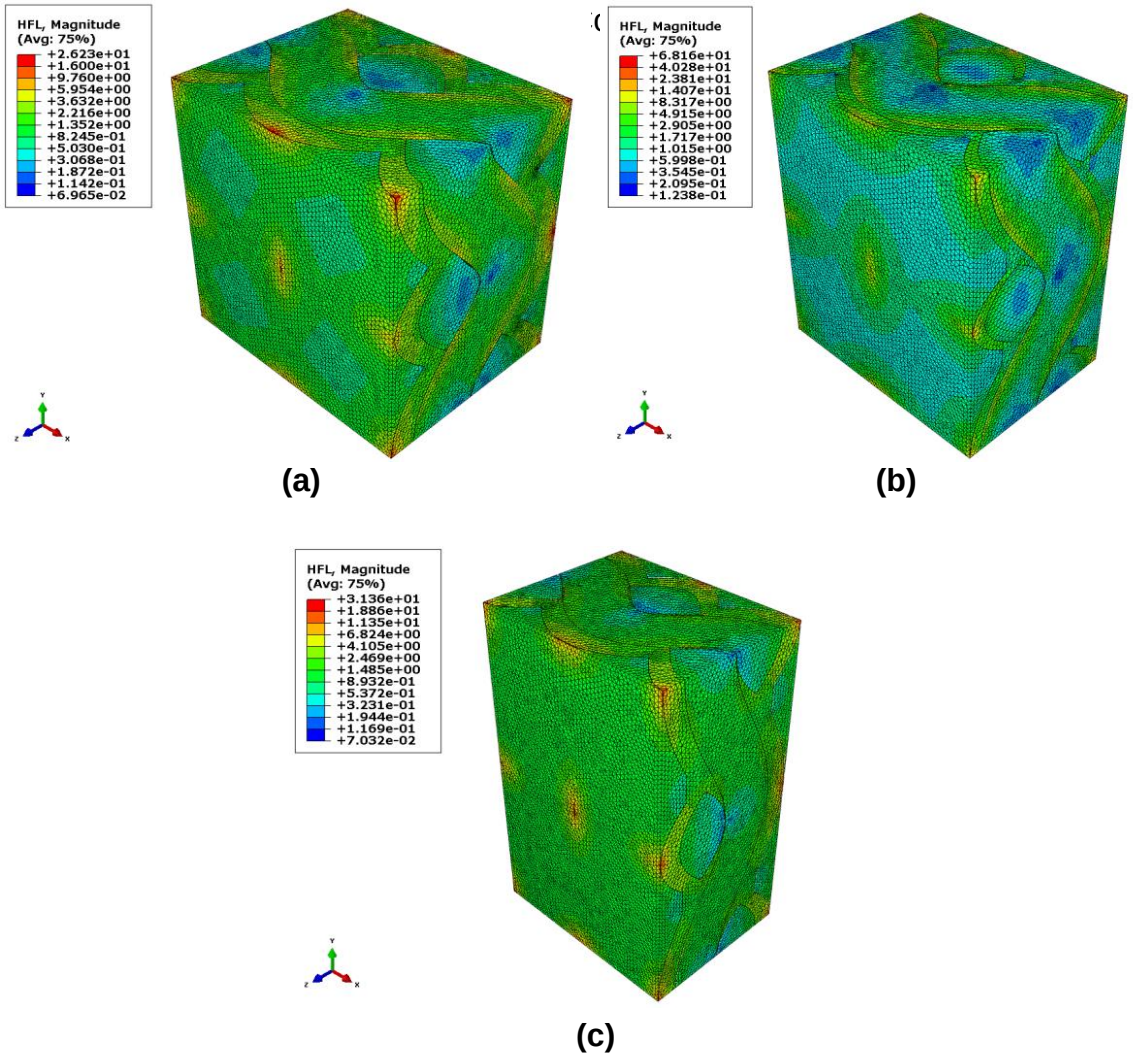

4. Experiment and Model Validation

Figure 10 shows the heat flow of the three MicroPCMSs coated fabric using DSC . In order to validate the simulated results tests were conducted to determine the thermal conductivity of MicroPCMs coated fabrics. Figure 11 shows the model of a developed thermal conductivity instrument, comprising of heater, hot and cold plates, heat flux sensor, fan heat sink, PID controller, thermocouple, multi-meter, AC/DC power supply and step down transformer. Fabric Samples are placed between the two plates with the lower plate heated by the controlled heater. Temperature sensor (thermocouple) is attached on the surface of the plates which monitors the temperate (T_1).The upper plate is attached with the heat flux senor, it is cooled by fan heat sink and another temperature sensor is connected at the surface of the cold plate which monitors the temperature (T_2). The temperature gradient (T_1-T_2) between the hot and cold plate allows the heat to flow from hot plate to cold plate through the fabric sample. The thermal conductivity of fabric samples are calculated by the following relation:

$$Keff = \frac{V}{S} \cdot \frac{t}{T_1 - T_2} \tag{10}$$

where V is the output of heat flux sensor, S heat flux sensor sensitivity, t is the sample thickness, T_1 is the hot plate temperature and T_2 is cold plate temperature.

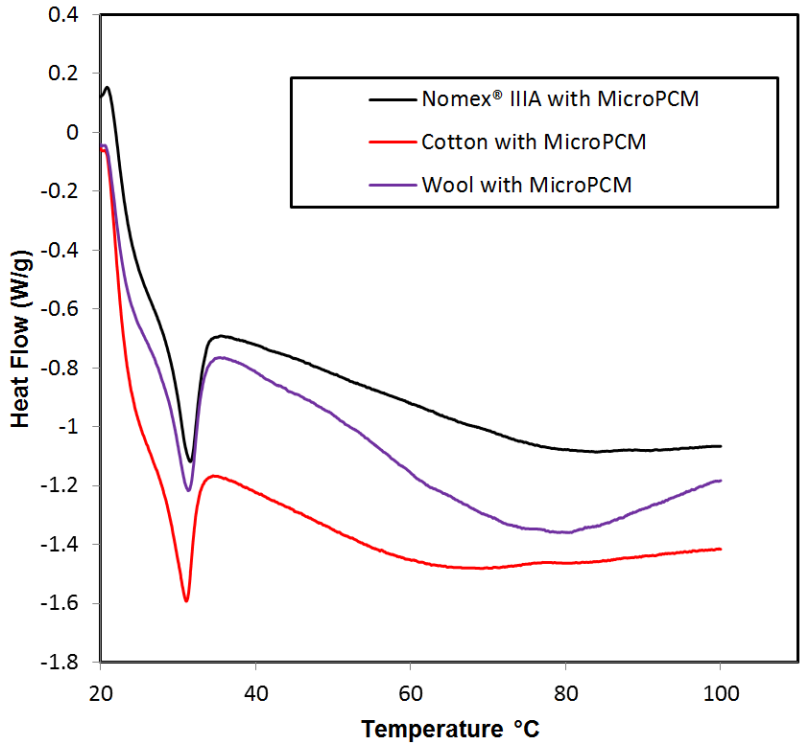

Figure 10. DSC Curves of MicroPCMs Coated Fabric

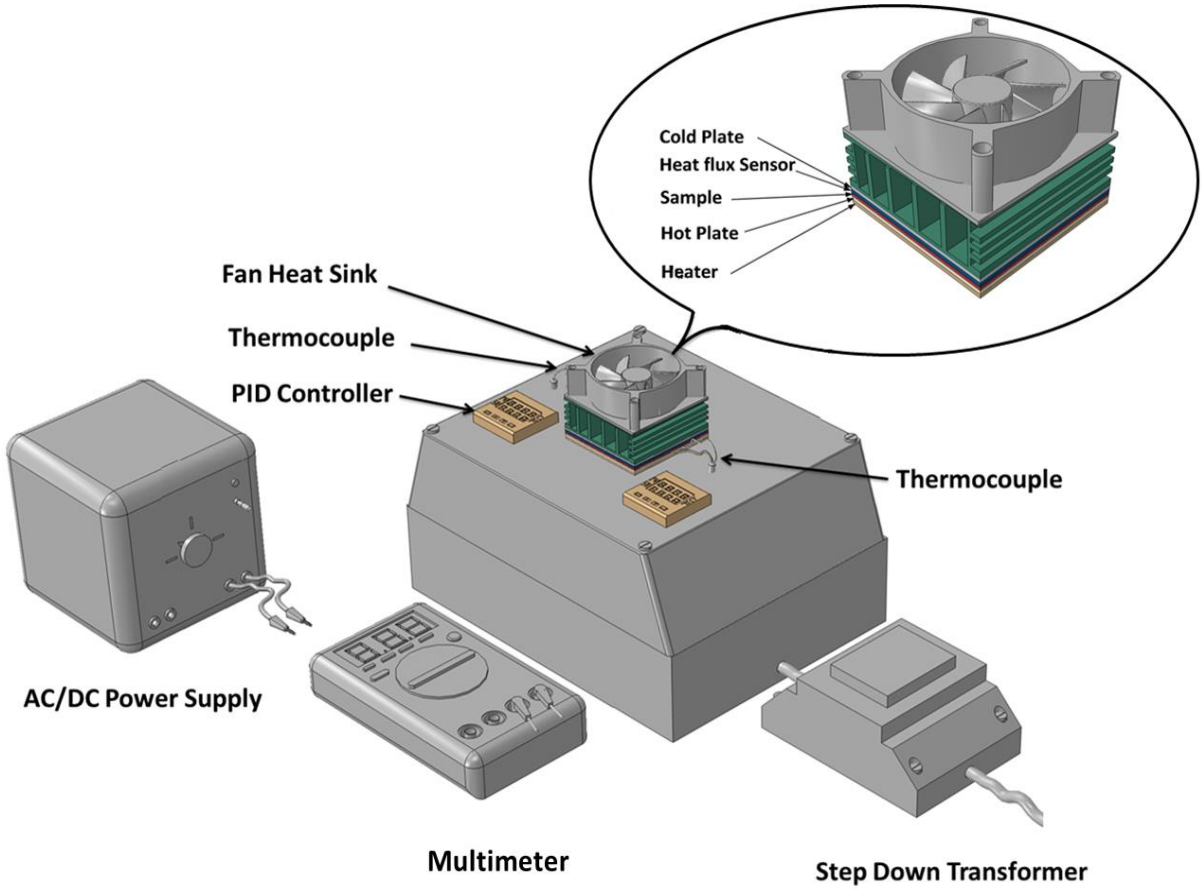

Figure 11. Schematic Diagram of Thermal Conductivity Experimental Setup

Table 7 shows the effective thermal conductivity obtained by experiment and finite element method. Figure 13 illustrats the correlation of thermal conductivity between experimental results which obtained from designed experimental setup and finite element method, R^2 and mean absolute error 6.11% shows the strong correlation between experimental and predicted results.

Table 7. Effective thermal conductivity values obtained from Experiment and FEM

Samples	Experimental effective thermal conductivity of MicroPCMs Coated Fabric K_{eff} (W/m.K)	Predicted effective thermal conductivity of MicroPCMs Coated Fabric K_{eff} (W/m.K)
Nomex® III	0.089	0.085
Cotton	0.087	0.081
Wool	0.072	0.077

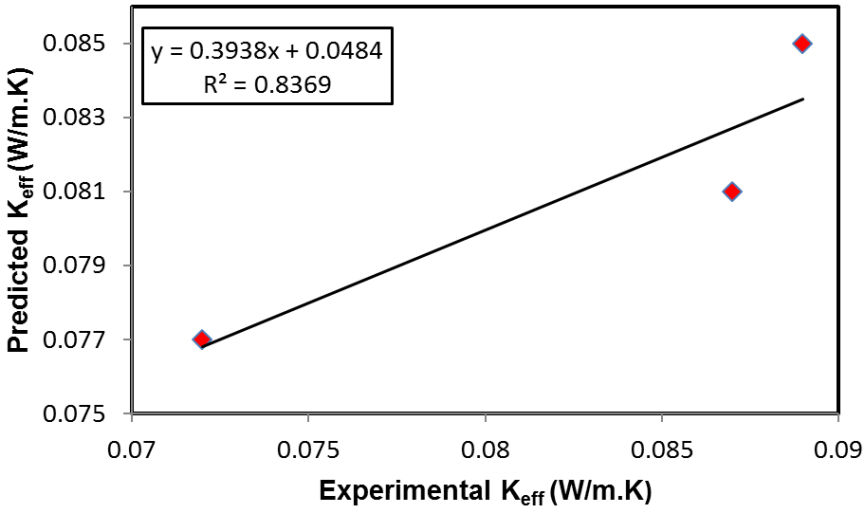

Figure 12. A Comparison of effective thermal conductivity between FE model predicttion and experiment.

5. conclusion

In this work a method is developed to predict the thermal conductivity of MicroPCMs coated fabrics by considering:

- conduction is the only mode of heat transfer;
- neglect the effect of internal heat generation; and
- PCM density variation with respect to temperature variation and entrapped air between the fabric surface and plates by using finite element method.

A strong correlation and small mean absolute error shows the applicability of method for the prediction of thermal conductivity of MicroPCMs coated fabric.

ACKNOWLEDGEMENT

The research is funded by NED University of Engineering and Technology, Karachi, Pakistan.

REFERENCES

[1] L.F. Cabezaa, C. Castellóna, M. Noguésa, M. Medranoa, R. Leppersb, O. Zubillagac, Energy and Buildings, 39 (2007) 113-119.
[2] R.C. Brown, J.D. Rasberry, S.P. Overmann, Powder Technology, 98 (1998) 217–222.
[3] M.N.A. Hawlader, M.S. Uddin, M.M. Khinb, Applied Energy, 74 (2003) 195–202.
[4] M.J. Huang, P.C. Eames, S. McCormack, P. Griffiths, N.J. Hewitt, Renewable Energy, 36 (2011) 2932–2939.
[5] F. Salaüna, E. Devauxa, S. Bourbigota, P. Rumeaud, Thermochimica Acta, 506 (2010) 82–93.
[6] N. Sarier, E. Onder, Thermochimica Acta, 454 (2007) 90-98.
[7] X.-X. Zhang, X.-C. Wang, X.-M. Tao, K.-L. Yick, Textile Research Journal, 76 (2006) 351-359
[8] M. Jiang, X. Song, G. Ye, J. Xu, Composites Science and Technology, 68 (2008) 2231–2237.
[9] Y.G. Bryant, D.P. Colvin, in: Techtextil-Symposium, 1992, pp. 1-8.
[10] K. Ghali, N. Ghaddar, B. Jones, Phase change in fabrics in: N. Pan, P. Gibson (Eds.) Thermal and moisture transport in fibrous materials, Woodhead Publishing Limited, North America, 2006, pp. 402-423.
[11] G.E.R. Lamb, K. Duffy-Morris, Textile Research Journal, 60 (1990) 261-265
[12] B. Pause, Journal of Industrial Textiles, 25 (1995) 59-68.
[13] M.L. Nuckols, Ocean Engineering, 26 (1999) 547–564.
[14] J. Kim, G. Cho, Textile Research Journal, 72 (2002) 1093-1098.
[15] K. Ghali, N. Ghaddar, J. Harathani, B. Jones, Textile Research Journal, 74 (2004) 205-214.
[16] Y. LI, Q. ZHU, Textile Research Journal, 74 (2004) 447-457
[17] L. Fengzhi, L. Yi, Modelling and Simulation in Materials Science and Engineering, 15 (2007) 223-235.
[18] L. Fengzhi, Modern Physics Letters B, 23 (2009) 501−504.
[19] B.-a. Ying, Y. Li, Y.-L. Kwok, Q.-w. Song, in: Information Engineering and Computer Science, 2009. ICIECS 2009. International Conference on, 2009, pp. 1-4.
[20] B. Wiesława, W. Henryk, FIBRES & TEXTILES in Eastern Europe, 17 (2009) 87-91.
[21] P. Sánchez, M.V. Sánchez-Fernandez, A. Romero, J.F. Rodríguez, L. Sánchez-Silva, Thermochimica Acta, 498 (2010) 16-21.
[22] S. Alay, C. Alkan, F. Göde, Journal of The Textile Institute, 103 (2011) 757-765.
[23] H. Yoo, J. Lim, E. Kim, Textile Research Journal, 83 (2013) 671-682.
[24] Y. Hu, D. Huang, Z. Qi, S. He, H. Yang, H. Zhang, Heat Mass Transfer, 49 (2013) 567-573.
[25] X.X. Zhang, Y.F. Fan, X.M. Tao, K.L. Yick, Materials Chemistry and Physics, 88 (2004) 300-307.
[26] W. Li, J. Wang, X. Wang, S. Wu, X. Zhang, Colloid Polym Sci, 285 (2007) 1691-1697.
[27] Z. Chen, G. Fang, Renewable and Sustainable Energy Reviews, 15 (2011) 4624-4632.
[28] W. Martienssen, H. Warlimont, Handbook of Condensed Matter and Materials Data, Springer Berlin Heidelberg, 2005.
[29] A.P. Drin, V.V. Efanova, N.I. Shut, Journal of Engineering Physics and Thermophysics, 66 (1994) 164.
[30] E.C. Guyer, D.L. Brownell, Handbook of applied thermal design, McGraw-Hill, New York, 1988.
[31] J.C. Maxwell, A treatise on electricity and magnetism, , 3rd ed., Dover, New York, 1954.
[32] M.W. Futschik, L.C. Witte, Arnerican Society of Mechanical Engineers, 271 (1994) 123-134.
[33] Morton, Hearle, Physical properties of textile fibres 4th ed., Woodhead, 2008.
[34] S. Kawabata, Journal of textile machine society of Japan, 39 (1986) 184-189.
[35] M.O.R. Siddiqui, D. Sun, Computational Materials Science, 75 (2013) 45-51.

Nomenclature

C_{pf}	fibre specific heat (J/kg.K)
ΔH_m	enthalpy of MicroPCMs (J/g)
ΔH_o	enthalpy of pure PCM (J/g)
d	diameter (µm)
K	thermal conductivity (W/m.K)
K_{air}	thermal Conductivity of air (W/m.K)
K_e	effective thermal conductivity of binder and MicroPCMs (W/m.K)
K_p	thermal conductivity of MicroPCMs (W/m.K)
K_{fa}	thermal conductivity of fibre in axial direction (W/m.K)
K_{ft}	thermal conductivity of fibre in transverse direction (W/m.K)
K_{ya}	axial thermal Conductivity of yarn (W/m.K)
K_{yt}	transverse thermal Conductivity of yarn (W/m.K)
Q_z	heat flux in z-direction
s	heat flux sensor sensitivity
t	sample thickness
T_1	hot plate temperature
T_2	cold plate temperature.
ΔT_z	temperature gradient in z-direction
T	thickness (µm)
V	output of heat flux sensor
V_{fy}	yarn fibre volume fraction

Greek Letters

α	mass fraction
ϕ	volume fraction
ρ	density (Kg/m^3)

Subscript

b	base material
c	core material
f	fibre
p	particle
s	shell